# Turing patterns via pinning control in the simplest memristive cellular nonlinear networks

Cite as: Chaos **29**, 103145 (2019); https://doi.org/10.1063/1.5115131
Submitted: 14 June 2019 . Accepted: 07 October 2019 . Published Online: 29 October 2019

Arturo Buscarino, Claudia Corradino, Luigi Fortuna, and Mattia Frasca

Chaos ARTICLE scitation.org/journal/cha

# Turing patterns via pinning control in the simplest memristive cellular nonlinear networks

Cite as: Chaos **29**, 103145 (2019); doi: 10.1063/1.5115131
Submitted: 14 June 2019 · Accepted: 7 October 2019 ·
Published Online: 29 October 2019



Arturo Buscarino,[1,2,a)] Claudia Corradino,[1,3] Luigi Fortuna,[1,2] and Mattia Frasca[1,2]

## AFFILIATIONS

[1]Dipartimento di Ingegneria Elettrica Elettronica e Informatica, University of Catania, Viale A. Doria 6, 95125 Catania, Italy
[2]CNR-IASI, Italian National Research Council—Institute for Systems Analysis and Computer Science "A. Ruberti", Via dei Taurini 19, 00185 Rome, Italy
[3]Istituto Nazionale di Geofisica e Vulcanologia, Piazza Roma 2, 95125 Catania, Italy

[a)]**Electronic mail:** arturo.buscarino@unict.it

## ABSTRACT

Complex patterns are commonly retrieved in spatially-extended systems formed by coupled nonlinear dynamical units. In particular, Turing patterns have been extensively studied investigating mathematical models pertaining to different fields, such as chemistry, physics, biology, mechanics, and electronics. In this paper, we focus on the emergence of Turing patterns in memristive cellular nonlinear networks by means of spatial pinning control. The circuit architecture is made by coupled units formed by only two elements, namely, a capacitor and a memristor. The analytical conditions for which Turing patterns can be derived in the proposed architecture are discussed in order to suitably design the circuit parameters. In particular, we derive the conditions on the density of the controlled nodes for which a Turing pattern is globally generated. Finally, it is worth to note that the proposed architecture can be considered as the simplest ideal electronic circuit able to undergo Turing instability and give rise to pattern formation.



**Since the seminal work on morphogenesis in biological organisms proposed by Alan Turing,[1] many efforts have been devoted to fully understand the mechanisms leading to pattern formation in areas such as biology and chemistry. Pattern formation in spatially-extended systems has also been investigated in fields far from biology, namely, mechanics,[2] electronics,[3,4] and thermodynamics.[5] These studies are based on the use of models belonging to a class of nonlinear differential equations, known as reaction-diffusion models, adopted to mimic the dynamics of spatially-extended systems in which a competitive inhibition-activation effect occurs. The necessary conditions for which Turing patterns may occur have extensively been discussed in several works.[3,4] These conditions guarantee the occurrence of the so-called Turing instability, i.e., the scenario in which the reactive cell admits a stable equilibrium point, which is made unstable by a diffusion-driven process. However, satisfying such conditions may be prevented by cell structure and parameters and/or the given coupling structure. In this paper, we introduce a novel strategy based on pinning control[6] to attain the condition for Turing instability, showing that the strategy is effective even acting at local scales.**

## I. INTRODUCTION

A fundamental issue in understanding the formation of spatial patterns in active media is the analysis and characterization of the diffusion processes which are at the basis of the morphogenesis.[1] The active medium is spatially discretized in cells, which are the basic units of the reaction-diffusion model. The dynamics of these cells is usually described as a second-order system, where the state variables represent the concentrations of two morphogenes[1] in the given cell. Diffusion takes place in the presence of a gradient in the morphogene concentrations. In particular, self-diffusion occurs if one morphogene induces a flux of the same morphogene; otherwise, when different chemical species are actually diffusing, a cross-diffusion process occurs. Although cross-diffusion is usually neglected, in many natural systems it is shown to play a central role.[7]

The paradigm of cellular nonlinear networks (CNNs) has widely been explored in the past to study spatiotemporal phenomena, including Turing patterns and autowaves formation.[3] Each cell of a CNN, in fact, embeds the dynamical behavior of a reactive element, and the coupling structure can implement self- and cross-diffusion processes. Recently, evidence of Turing pattern formation has been

presented in a CNN with cross-diffusion.[8] The cells of that structure incorporate memristors, thus leading to a so-called memristive CNN (MCNN).

The memristor is a two-terminal electronic device displaying a functional relationship between the time integral of the current through it and that of the voltage across its terminals. It has theorized in 1971[22] and, recently, thanks to the experimental evidence of its existence,[9] has been intensively investigated as a fundamental element for dynamical nonlinear systems. Different models of the memristive devices have been formulated, either based on the physics of the device or on the representation of the functional relationship between flux and charge. Furthermore, the nonlinearity has been modeled by means of piecewise linear[10] or more sophisticated functions.[11,12] This device has gained interest in electronic and neuroscience community,[9–13] since its characteristic of being a nonlinear and memory element make it suitable in the search of simple chaotic circuits.[14] Moreover, it has been shown that MCNNs are suitable to generate spatiotemporal phenomena such as autowaves.[15]

A reaction-diffusion system exhibits Turing patterns in the presence of a diffusion-driven instability, when the equilibrium solution of the isolated cell is stable to small perturbations but unstable when diffusion is present. In the case of the MCNN presented in Ref. 8, the diffusion process needed to satisfy the Turing conditions must include both self-diffusions and cross-diffusions. Here, we introduce a novel strategy based on the application of the pinning control approach with the aim of obtaining Turing patterns in systems whose parameters without control do not satisfy Turing conditions.

Pinning control[6] represents a well known technique which, by acting on a selected subset of nodes in a complex network, aims at achieving a global objective, i.e., the control of the global behavior of the system. In this paper, we adopt such strategy with the aim of applying a local permanent negative feedback loop to a fraction of cells, thus locally satisfying Turing conditions. The strategy should be effective also when pinning a small fraction of cells in the MCNN, thus providing the possibility to control Turing pattern emergence in a MCNN where the majority of the cells does not satisfy Turing conditions. It will be shown that the diffusion coefficients of the MCNN play a crucial role in the fraction of cells that must be pinned to attain Turing patterns; the higher are the strengths, the lower is the number of pinned nodes.

The paper is organized as follows: in Sec. II, the MCNN based on a novel simplified cell is introduced; in Sec. III, the conditions for the emergence of Turing patterns in the proposed MCNN system are determined; in Sec. IV, numerical results are presented showing the different types of Turing patterns that can be observed in the MCNN; in Sec. V, the conclusions are reported.

## II. THE MEMRISTIVE CELLULAR NONLINEAR NETWORK

The MCNN discussed in the following represents an active medium discretized in a lattice of $N \times N$ basic cells. The basic cell is the simple electronic circuit shown in Fig. 1, it is composed of the parallel of two basic components: a capacitor (linear and passive) and a memristor system,[14] whose model is defined by the following

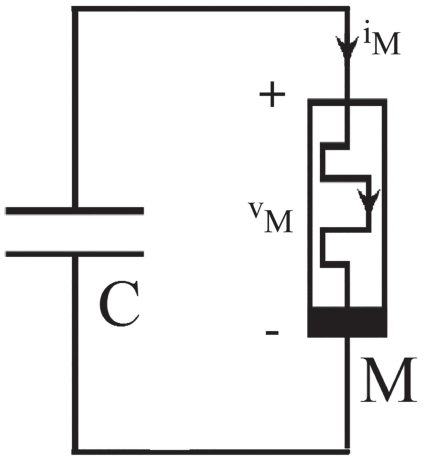


**FIG. 1.** Schematic representation of the memristor-capacitor circuit.

equations:

$$\begin{aligned} i_M &= M(\phi)v_M = \beta(\phi^2 - 1)v_M, \\ \dot{\phi} &= f_M(\phi, v_M) = v_M - \alpha\phi - v_M\phi, \end{aligned} \tag{1}$$

where $v_M$ and $i_M$ are the voltage and the current, respectively, associated with the memristor system; $\phi$ is the internal state, i.e., the flux $f_M(\phi, v_M)$ is the internal state function; and $M(\phi) = \frac{dq(\phi)}{d\phi}$ is the memductance of the memristive system, relating memristor current and voltage. Furthermore, $\alpha$ and $\beta$ are memristor parameters, defining the internal state dynamics, according to the form proposed in Ref. 14.

Applying the standard Kirchhoff's laws to the circuit in Fig. 1, and recalling the memristor constitutive relationship in Eq. (1), the following equations are derived:

$$\begin{aligned} C\dot{v} &= -\beta(\phi^2 - 1)v, \\ \dot{\phi} &= v - \alpha\phi - v\phi, \end{aligned} \tag{2}$$

where $v$ is the voltage across both the capacitor $C$ and the memristor $M$ and $\phi$ is the flux associated with the memristor. Introducing the variables $x = v$, $y = \phi$, and the parameter $\gamma = \frac{1}{C}$, Eq. (2) can be rewritten as

$$\begin{aligned} \dot{x} &= -\gamma\beta(y^2 - 1)x, \\ \dot{y} &= x - \alpha y - xy. \end{aligned} \tag{3}$$

The $N \times N$ MCNN is obtained by considering the circuit equations (3) as the model governing each cell of the grid and connecting them according to a diffusive coupling, which locally connects them with their four nearest neighbors as

$$\begin{aligned} \dot{x}_{i,j} &= f(x_{i,j}, y_{i,j}) + D_{11}\nabla^2 x_{i,j}, \\ \dot{y}_{i,j} &= g(x_{i,j}, y_{i,j}) + D_{22}\nabla^2 y_{i,j}, \end{aligned} \tag{4}$$

where $i$ and $j$ represent the indices of the row and the column and $D_{11}$ and $D_{22}$ are the self-diffusion coefficients. $f(x, y) = -\gamma\beta(y^2 - 1)x$

and $g(x,y) = x - \alpha y - xy$, and $\nabla^2$ is the two-dimensional discrete Laplacian operator,

$$\begin{aligned}\nabla^2 x_{i,j} &= x_{i+1,j} + x_{i-1,j} + x_{i,j-1} + x_{i,j+1} - 4x_{i,j},\\ \nabla^2 y_{i,j} &= y_{i+1,j} + y_{i-1,j} + y_{i,j-1} + y_{i,j+1} - 4y_{i,j}.\end{aligned} \tag{5}$$

In addition, in the following the partial derivatives of the functions $f(x,y)$ and $g(x,y)$ will be denoted by $f_x = \frac{\partial f}{\partial x}, f_y = \frac{\partial f}{\partial y}, g_x = \frac{\partial g}{\partial x}$, and $g_y = \frac{\partial g}{\partial y}$.

In the view of an implementation of the proposed MCNN, it should be noted that the coupling scheme can be realized introducing linear resistors as concerns voltage diffusion, while flux diffusion strongly depends on the specific realization of the memristor. In some VLSI implementations, in fact, memristor fluxes can be coupled by fabricating the device in nearby regions of the integrated circuit.[16,17] Considering, instead, a practical implementation based on off-the-shelf discrete components, Eq. (4) can be realized, for example, following a state variable approach,[18] in which each state variable is associated with a voltage across a capacitor. In this case, the diffusion process can be implemented by means of linear resistors.

## III. TURING CONDITIONS

In order to check whether a reaction-diffusion system may exhibit Turing patterns, that is, diffusion-driven instability, the stability of the equilibrium point of the isolated cell has to be investigated so that to verify that, if it is stable, it is driven to instability when the diffusion process takes place.[4] This principle is translated into mathematical conditions by first considering the cell as isolated, linearizing the dynamics around its equilibrium and studying the stability of its equilibrium point through the analysis of the Jacobian matrix. A first set of conditions is, thus, obtained by imposing that the isolated cell admits a stable equilibrium point. Then, the effect of the diffusion is considered through a technique based on the evaluation of the spatial eigenvalues, which allows to consider the effect of the coupling, deriving the conditions on the parameters such that the equilibrium point becomes unstable.[19] In this section, this approach is applied to the MCNN in Eq. (4) in order to derive the conditions in the parameter space leading to Turing patterns.

The isolated cell described by Eq. (3) admits two equilibrium points, one located at the origin $Q_0 = (0,0)$ and the other in $Q_1 = (-\frac{\alpha}{2}, -1)$. With the aim of studying the stability of a generic equilibrium point of system (3), let us indicate it as $(\bar{x},\bar{y})$and compute the Jacobian matrix

$$\mathrm{A} = \begin{bmatrix} f_x & f_y \\ g_x & g_y \end{bmatrix} = \begin{bmatrix} -\gamma\beta(\bar{y}^2 - 1)\bar{x} & -2\gamma\beta\bar{y}\bar{x} \\ 1 - \bar{y} & -\alpha - \bar{x} \end{bmatrix}_{(\bar{x},\bar{y})}, \tag{6}$$

where without lack of generality we took $\gamma = 1$. Indicating with

$$\begin{aligned}\mathrm{tr(A)} &= (f_x + g_y)|_{(\bar{x},\bar{y})} = \beta(1 - \bar{y}^2) - \alpha - \bar{x},\\ \det(\mathrm{A}) &= (f_x g_y - f_y g_x)|_{(\bar{x},\bar{y})} = \beta(\bar{y} - 1)[(\alpha - \bar{x})(\bar{y} + 1) - 2\bar{x}\bar{y}],\end{aligned} \tag{7}$$

the characteristic polynomial of matrix A takes the following form

$$\lambda^2 - \mathrm{tr(A)}\lambda + \det(\mathrm{A}) = 0. \tag{8}$$

The equilibrium point $(\bar{x},\bar{y})$ is, hence, stable if and only if $\mathrm{tr(A)} < 0$ and $\det(\mathrm{A}) > 0$. As a consequence, the first two conditions for Turing patterns when $(\bar{x},\bar{y})$=$Q_0$ are

$$\begin{aligned}\mathrm{tr(A)} &= \beta - \alpha < 0 (C_0.1),\\ \det(\mathrm{A}) &= -\alpha\beta > 0\ (C_0.2).\end{aligned} \tag{9}$$

Similarly, the first two conditions for Turing patterns when $(\bar{x},\bar{y}) = Q_1$ are

$$\begin{aligned}\mathrm{tr(A)} &= -\frac{\alpha}{2} < 0\ (C_1.1),\\ \det(\mathrm{A}) &= \alpha\beta > 0\ (C_1.2).\end{aligned} \tag{10}$$

Let us consider now the MCNN state equations (4). In order to obtain the conditions on the coupled system, Eqs. (4) are linearized around the generic equilibrium point $(\bar{x},\bar{y})$ of the isolated cell[3] obtaining

$$\begin{aligned}\dot{\tilde{x}}_{i,j} &= f_x\tilde{x}_{i,j} + f_y\tilde{y}_{i,j} + D_{11}\nabla^2\tilde{x}_{i,j},\\ \dot{\tilde{y}}_{i,j} &= g_x\tilde{x}_{i,j} + g_y\tilde{y}_{i,j} + D_{22}\nabla^2\tilde{y}_{i,j},\end{aligned} \tag{11}$$

where $\tilde{x}$ and $\tilde{y}$ represent the deviations from the equilibrium point. The properties of (11) are analyzed by the spatial eigenfunction-based decoupling approach. This approach has been introduced and formalized in Ref. 3 and allows to reduce the analysis of pattern formation in spatiotemporal systems to the analysis of an uncoupled system of two first-order linear differential equations directly related to the spatial eigenvectors. Therefore, a system of $2N^2$ coupled differential equations as $N^2$ decoupled systems of two differential equations. The main idea behind this approach is to find a solution of the MCNN as a weighted sum of $N^2$ orthonormal space-dependent eigenfunctions $\phi_{N^2}(m,n,i,j)$ associated with the discrete Laplacian operator,

$$\begin{aligned}\nabla^2\phi_{N^2}(m,n,i,j) &= \phi_{N^2}(m,n,i+1,j) + \phi_{N^2}(m,n,i-1,j)\\ &\quad + \phi_{N^2}(m,n,i,j+1) + \phi_{N^2}(m,n,i,j-1)\\ &\quad - 4\phi_{N^2}(m,n,i,j) = -k^2_{mn}\phi_{N^2}(m,n,i,j),\end{aligned} \tag{12}$$

where $k^2_{mn}$ are the corresponding spatial eigenvalues and the form of $\phi_{N^2}(m,n,i,j)$ depends on the boundary conditions.[3]

If one of these modes $k^2_{mn}$ leads to an unstable equilibrium point, diffusion-driven instability is induced. To check the occurrence of this condition, the stability of the equilibrium point of the cell in the presence of diffusion is studied with respect to the spatial eigenvalues that will be generically named as a generic variable $k^2$, thus neglecting which specific mode becomes unstable. Hence, in the following equations, the index $mn$ will be dropped. Therefore, the stability of the generic equilibrium point when diffusion is present depends on the following Jacobian matrix:

$$\mathrm{J} = \mathrm{A} - k^2\mathrm{D} = \begin{bmatrix} -\beta(\bar{y}^2 - 1) - k^2 D_{11} & -2\beta\bar{y}\bar{x} \\ 1 - \bar{y} & -\alpha - \bar{x} - k^2 D_{22} \end{bmatrix}, \tag{13}$$

where $k^2$ is the spatial eigenvalue and $\mathrm{D} = \begin{bmatrix} D_{11} & 0 \\ 0 & D_{22} \end{bmatrix}$ is the diffusion coefficients matrix. It is worth to note that, in the definition

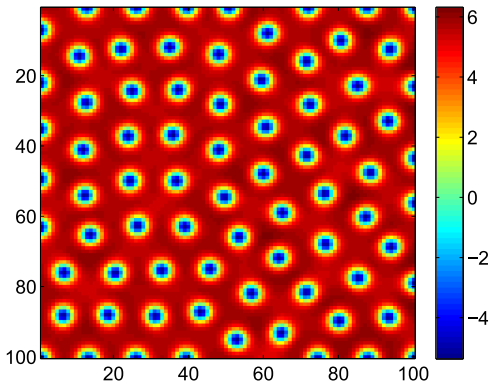


(a)

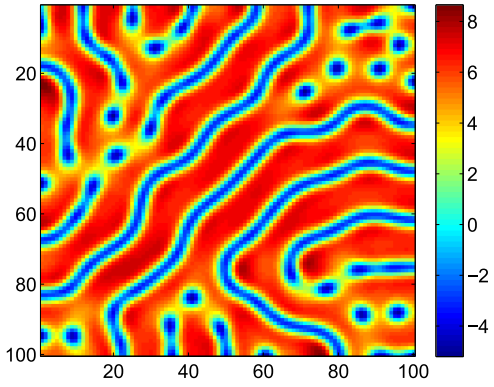


(b)

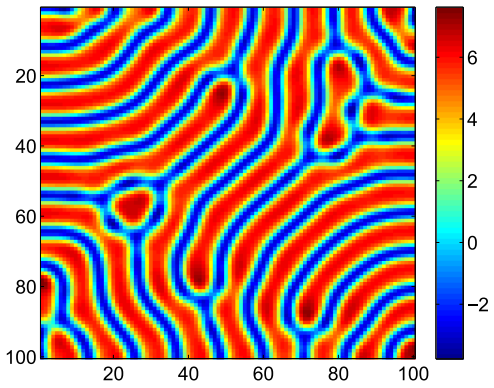


(c)

**FIG. 2.** Turing patterns generated by a 100 × 100 MCNN as in Eq. (4) in layer $x$, where $\eta$ assumes three different values: (a) $\eta = 1.8$, spots, (b) $\eta = 1.9$, mixture of stripes and spots, (c) $\eta = 2$, stripes. The other parameters are fixed as $\alpha = 1.6$, $\beta = 0.06$, $D_{11} = 0.5$, and $D_{22} = 10$. Without loss of generality, initial conditions are taken randomly from a normal distribution with zero mean and unitary variance, zero-flux boundary conditions are considered.

of the diffusion process, we take into consideration the presence of self-diffusion coefficients only.

The conditions for Turing instability require that the Jacobian matrix J admits at least an unstable eigenvalue. This implies that $\mathrm{tr(J)} > 0$ or $\det(\mathrm{J}) < 0$. In our case, the trace and the determinant of J are

$$\begin{aligned} \mathrm{tr(J)} &= -k^2(D_{11} + D_{22}) + \mathrm{tr(A)}, \\ \det(\mathrm{J}) &= -(D_{22}f_x + D_{11}f_y)k^2 + \det(D)k^4 + \det(\mathrm{A}). \end{aligned} \tag{14}$$

By considering $Q_0$, the following equations are obtained:

$$\begin{aligned} \mathrm{tr(J)} &= -k^2(D_{11} + D_{22}) - \alpha + \beta, \\ \det(\mathrm{J}) &= (D_{11}D_{22})k^4 - (-\alpha D_{11} + \beta D_{22})k^2 - \alpha\beta. \end{aligned} \tag{15}$$

As concerns tr(J), according to condition $C_0.1$ in Eq. (9) the trace of A is negative and $-k^2(D_{11} + D_{22})$ is negative too. This yields that their sum, i.e., tr(J), is also negative. Therefore, Turing instability can occur only if $\det(\mathrm{J}) < 0$ for some value of $k^2$. Since $\det(\mathrm{D}) = D_{11}D_{22} > 0$ (in order to have a passive diffusion coupling) and $C_0.2$ in Eq. (9) implies that $-\alpha\beta > 0$, we get that $\alpha > 0$ and $\beta < 0$. Thus, the first required condition is $-\alpha D_{11} + \beta D_{22} > 0$ that can never be met since diffusion coefficients are always positive quantities. As a consequence, Turing pattern conditions cannot be satisfied for $Q_0$.

Let us now consider $Q_1$, the following equations hold:

$$\begin{aligned} \mathrm{tr(J)} &= -k^2(D_{11} + D_{22}) - \frac{\alpha}{2}, \\ \det(\mathrm{J}) &= (D_{11}D_{22})k^4 - \left(-\frac{\alpha}{2}D_{11}\right)k^2 + 2\alpha\beta. \end{aligned} \tag{16}$$

Even in this case, as concerns tr(J), according to condition $C_1.1$ in Eq. (10) the trace of A is negative and $-k^2(D_{11} + D_{22})$ is negative too. This yields that their sum, i.e., tr(J), is also negative. Therefore, Turing instability can occur only if $\det(\mathrm{J}) < 0$ for some value of $k^2$. To this aim, since $\det(\mathrm{D}) = D_{11}D_{22} > 0$ (in order to have a passive diffusion coupling) and $\alpha\beta > 0$ in virtue of $C_1.2$ in Eq. (10), a first condition is $-\frac{\alpha}{2}D_{11} > 0$ that can never be met. Therefore, in this scenario, Turing patterns cannot emerge for all configuration of the system parameters, unless cross-diffusions terms are considered. In this case, in fact, Turing conditions for equilibrium point $Q_0$ can be satisfied.

In order to avoid the presence of cross-diffusions and simplify the coupling needed to attain Turing patterns, we propose an approach that exploits the so-called spatial pinning control[20,21] in order to allow global Turing pattern emergence. In particular, we introduce a feedback control that is applied to a given cell with some probability $\bar{p}$ and remains active for the whole duration of the numerical simulation. In this case, the equations of the single cell will change as follows:

$$\begin{aligned} \dot{x}_{ij} &= -\gamma\beta(y_{ij}^2 - 1)x_{ij} + u_{ij}, \\ \dot{y}_{ij} &= x_{ij} - \alpha y_{ij} - x_{ij}y_{ij}, \end{aligned} \tag{17}$$

where $u_{ij} = -\xi_{ij}\eta y_{ij}$ is the local linear negative feedback control law, with $\eta$ indicating the control strength and $\xi_{ij}$ is defined as follows:

$$\xi_{ij} = \begin{cases} 1 \text{ with probability } \bar{p}, \\ 0 \text{ with probability } 1 - \bar{p}. \end{cases}$$

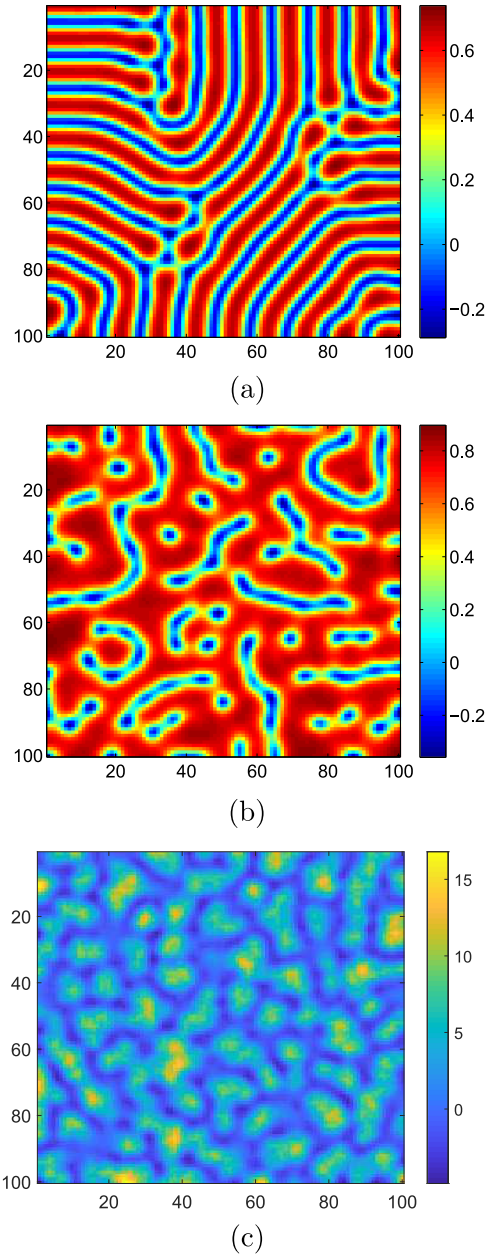


**FIG. 3.** Turing patterns generated by a 100 × 100 MCNN as in Eq. (4) in layer $y$: (a) and(b) effect of the probability $\bar{p}$ on the pattern shape. Parameters are (a) $\eta = 2.2$ and $\bar{p} = 1$, (b) $\eta = 2.2$ and $\bar{p} = 0.9$, and (c) $\eta = 3.5$ and $\bar{p} = 0.75$. Other parameters as indicated in the text.

The corresponding MCNN equations are

$$\begin{aligned} \dot{x}_{i,j} &= -\gamma\beta(y_{i,j}^2 - 1)x_{i,j} + u_{i,j} + D_{11}\nabla^2 x_{i,j}, \\ \dot{y}_{i,j} &= x_{i,j} - \alpha y_{i,j} - x_{i,j}y_{i,j} + D_{22}\nabla^2 y_{i,j}. \end{aligned} \tag{18}$$

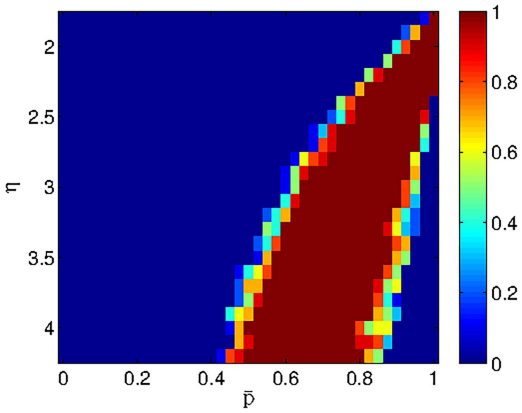


**FIG. 4.** Effect of $\eta$ and $\bar{p}$ on pattern emergence. Other parameters are fixed as $\alpha = 1.6$, $\beta = 0.6$, $D_{11} = 0.5$, and $D_{22} = 10$.

The control action can be considered as a flux-controlled current source injecting in the cell a current proportional to the flux of the memristor.

We start applying the feedback control to each cell of the MCNN, namely, $\bar{p} = 1$, i.e., $\xi_{ij} = 1$ for each node $(i, j)$ of the MCNN. Thus, the Turing conditions of the cell described by Eq. (17) and those of the MCNN described by Eq. (18) when $\xi_{ij} = 1$ are retrieved following the same steps previously described obtaining the following conditions:

$$\alpha - \beta > 0, \tag{C1}$$

$$-\alpha\beta - \eta > 0, \tag{C2}$$

$$-\alpha D_{11} + \beta D_{22} > 0, \tag{C3}$$

$$(-\alpha D_{11} - \beta D_{22})^2 - 4\det(D)(-\alpha\beta - \eta) > 0, \tag{C4}$$

$$\det(\mathrm{D}) = D_{11}D_{22} > 0, \tag{C5}$$

which are derived when the equilibrium point of the isolated cell in Eq. (17) is $Q_0 = (0, 0)$.

Thanks to the action of the control law, Turing conditions can now be met by properly selecting the control strength $\eta$, since condition (C4) can now be satisfied, thus leading to the generation of Turing patterns. This analysis thus indicates that controlling each cell of the network is effective for the goal of Turing Pattern formation; in Sec. IV, after presenting computational results confirming these theoretical considerations, we numerically investigate whether the same goal can be reached by applying control to a smaller fraction of the network nodes.

## IV. NUMERICAL RESULTS

Numerical simulations of the MCNN in Eq. (4) have been performed considering $N = 100$. Without loss of generality, the initial conditions for the variables $x_{i,j}$ and $y_{i,j}$ have been drawn from a normal distribution with zero mean and standard deviation equal to 1, and zero-flux boundary conditions are imposed. The first case

considered is when each cell of the MCNN is pinned, thus $\bar{p} = 1$. We discuss now the numerical results obtained from the integration of the MCNN for a specific set of parameters satisfying conditions (C1)–(C5), namely, $\alpha = 1.6$, $\beta = 0.6$, $D_{11} = 0.5$, $D_{22} = 10$ while varying $\eta$. Our results revealed that the strength of the feedback control action affects the final state of the MCNN, allowing a selection of the type of the emerging pattern.

Some examples are shown in Fig. 2 where spots [Fig. 2(a)], mixed [Fig. 2(b)], and stripes [Fig. 2(c)] like patterns are obtained by increasing $\eta$ ($\eta = 1.8$, $\eta = 1.9$, and $\eta = 2.1$, respectively). Notice that only layer $x$ is shown in Fig. 2.

In order to further investigate the capabilities of the pinning control action, we consider now the possibility of controlling a fraction of nodes in the MCNN, by decreasing the pinning probability $\bar{p}$ and of characterizing the effect of $\bar{p}$ on the pattern selection. In particular, as shown in Fig. 3, the kind of pattern changes from stripes to mixed when a smaller fraction of nodes are controlled, becoming more and more mixed and irregular while decreasing $\bar{p}$. Further decreasing $\bar{p}$ prevents the formation of patterns.

In order to characterize the effect of varying the control parameters $\bar{p}$ and $\eta$, we performed a statistic analysis on the emergence of Turing patterns over 100 realizations. In Fig. 4, the percentage of realizations leading to Turing pattern in the parameter space $\eta - \bar{p}$ is shown, according to the reported colorbar.

## V. CONCLUSIONS

In this paper, the emergence of Turing patterns in a MCNN has been studied exploiting a novel spatial pinning control technique. The conditions to design the parameters of the memristive circuit, used as basic cell, have been analytically derived in accordance to the specific control law. Numerical simulations allowed to observe different types of patterns, including spots, stripes and mixed, by opportunely setting the parameter of the control law and the fraction of pinned nodes.

In the control scheme proposed in our paper, we took into consideration the inclusion of feedback term applied to the reactive part of the system. The control action is maintained during the whole dynamical process; thus, it does not act as a finite-amplitude perturbation. The mathematical effect of the control action is in fact the variation of one of the Jacobian elements. Moreover, the inclusion of the control action does not alter the stability of the isolated equilibrium point. Patterns obtained with the control action are, therefore, the result of the diffusion-driven instability solely and, hence, the arising spatial patterns are consistent with the TP scenario.

Despite the fact that the implementation of electronic circuits able to reproduce complex spatiotemporal patterns is a well established result, we investigated the possibility to drive a MCNN made by the simplest ideal circuital configuration toward the emergence of Turing patterns introducing a general technique to control the global behavior of the system by controlling locally a fraction of the nodes in the MCNN.

## REFERENCES


[1] A. Turing, "The chemical basis of morphogenesis," Philos. Trans. R. Soc. Lond. B Biol. Sci. **237**, 37–72 (1952).
[2] A. K. Harrisa, D. Stopak, and P. Warner, "Generation of spatially periodic patterns by a mechanical instability: A mechanical alternative to the turing model," J. Embryol. Exp. Morph. **80**, 1–20 (1984).
[3] L. Goras and L. O. Chua, "Turing patterns in CNNS. II. Equations and behaviors," IEEE Trans. Circuits Syst. I Fundam. Theory Appl. **42**, 612–626 (1995).
[4] L. Goras, L. O. Chua, and D. M. W. Leenaerts, "Turing patterns in CNNS. I. Once over lightly," IEEE Trans. Circuits Syst. I Fundam. Theory Appl. **42**, 602–611 (1995).
[5] U. Daybelge, C. Yarim, and A. Nicolai, "Spatiotemporal oscillations in tokamak edge layer and their generation by various mechanisms," in *Proceedings of the 24th IAEA Fusion Energy Conference* (IAEA, 2012).
[6] X. Li, X. Wang, and G. Chen, "Pinning a complex dynamical network to its equilibrium," IEEE Trans. Circuits Syst. I Reg. Papers **51**, 2074–2087 (2004).
[7] V. K. Vanag and I. R. Epstein, "Cross-diffusion and pattern formation in reaction-diffusion systems," Phys. Chem. Chem. Phys. **11**, 897–912 (2009).
[8] A. Buscarino, C. Corradino, L. Fortuna, M. Frasca, and L. Chua, "Turing patterns in memristive cellular nonlinear networks," IEEE Trans. Circuits Syst. I Reg. Papers **63**, 1222–1230 (2016).
[9] D. B. Strukov, G. S. Snider, D. R. Stewart, and R. S. Williams, "The missing memristor found," Nature **453**, 80–83 (2008).
[10] M. Itoh and L. O. Chua, "Memristor oscillators," Int. J. Bifurcat. Chaos **18**, 3183–3206 (2008).
[11] A. Buscarino, L. Fortuna, M. Frasca, and L. V. Gambuzza, "A chaotic circuit based on Hewlett-Packard memristor," Chaos **22**, 023136-1–023136-9 (2012).
[12] A. Buscarino, L. Fortuna, M. Frasca, and L. V. Gambuzza, "A gallery of chaotic oscillators based on HP memristor," Int. J. Bifurcat. Chaos **23**, 1330015-1–1330015-14 (2013).
[13] A. Ascoli, S. Slesazeck, H. Mahne, R. Tetzlaff, and T. Mikolajick, "Nonlinear dynamics of a locally-active memristor," IEEE Trans. Circuits Syst. I Reg. Papers **62**, 1165–1174 (2015).
[14] B. Muthuswamy and L. Chua, "Simplest chaotic circuit," Int. J. Bifurcat. Chaos **20**, 1567–1580 (2010).
[15] V. T. Pham, A. Buscarino, L. Fortuna, and M. Frasca, "Autowaves in memristive cellular neural networks," Int. J. Bifurcat. Chaos **22**, 1230027-1–1230027-9 (2012).
[16] V. Mladenov and S. Kirilov, "Analysis of the mutual inductive and capacitive connections and tolerances of memristors parameters of a memristor memory matrix," in *2013 European Conference on Circuit Theory and Design (ECCTD)* (IEEE, 2013), pp. 1–4.
[17] W. Cai and R. Tetzlaff, "Beyond series and parallel: Coupling as a third relation in memristive systems," in *2014 IEEE International Symposium on Circuits and Systems (ISCAS)* (IEEE, 2014), pp. 1259–1262.
[18] A. Buscarino, L. Fortuna, M. Frasca, and G. Sciuto, *A Concise Guide to Chaotic Electronic Circuits* (Springer, 2014).
[19] J. D. Murray, *Mathematical Biology. II Spatial Models and Biomedical Applications* (Springer-Verlag, 2001).
[20] M. Frasca, A. Buscarino, A. Rizzo, and L. Fortuna, "Spatial pinning control," Phys. Rev. Lett. **108**, 204102 (2012).
[21] W. Yu, G. Chen, J. Lu, and J. Kurths, "Synchornization via pinning control on general complex networks," SIAM J. Control Optim. **51**, 1395–1416 (2013).
[22] L. Chua, "Memristor: The missing circuit element," IEEE Trans. Circuit Theory **18**, 507–519 (1971).